Proc. of the European Safety and Reliability Conference (ESREL 2026)
Edited by José C. Matos, Paulo B. Lourenço, Michael Beer, Daniel Oliveira, Edoardo Patelli, Hélder S. Sousa, Rui A. Silva and Monica Santamaria
 Published by Research Publishing, Singapore.
doi: 10.3850/ESREL2026061419_esrel26-p26202-cd

Uncertainty And Sensitivity Analysis of the iRAP Road Safety Risk Assessment Model for Vehicles

Author's: Ameen, Horia *(Spain)1* horia.ameen@uvigo.gal;
Ghasemlou, Arshia *(Spain)1* arshia.ghasemlou@uvigo.gal;
Soilán, Mario *(Spain)1* msoilan@uvigo.gal;
Riveiro, Belen *(Spain)1* belenriveiro@uvigo.gal
Affiliaton's: 1 - CINTECX, GeoTECH group, Universidade de Vigo

Abstract: Roads are among the most vital infrastructures developed by humans, serving as the backbone of terrestrial transportation systems worldwide. Given their critical role, systematic evaluation of road hazards and associated risks has become a priority for governments and agencies that invest substantial resources in monitoring and improving road safety. To quantify these risks, the International Road Assessment Programme (iRAP) has proposed a standardized methodology and a comprehensive road safety risk score formula that incorporates numerous roadside and roadway attributes, such as geometry, roadside hazards, delineation quality, and protection measures. In this study, we apply a Monte Carlo simulation framework to the iRAP vehicle risk score formula to explore the uncertainty propagation and parametric influence of input variables. For the main analysis, we generated 32,768 simulated scenarios using a Sobol quasi–Monte Carlo design, covering the full spectrum of possible combinations of categorical and continuous attributes in a statistically representative manner. The sampling strategy was designed to ensure adequate coverage of both common and extreme road conditions, thereby capturing the realistic variability of field data. The resulting distribution of road risk scores was then analyzed to quantify expected ranges and probabilistic behavior under uncertain input conditions. Subsequently, sensitivity analysis was performed to identify the most influential parameters governing the final safety score. Both correlation-based (Spearman and Pearson) and variance-based (Sobol indices) techniques were employed to evaluate the relative contribution of each factor. The findings reveal the parameters that most critically affect the iRAP score, providing essential guidance for targeted interventions. Furthermore, the outcomes can be integrated into automated and AI-driven road assessment systems, enhancing their interpretability by quantifying how sensitive the computed risk score is to variations in specific attributes.
Keywords: Road safety risk assessment, Sensitivity analysis, Simulation-based analysis, Probabilistic modeling, Decision

1. Introduction

Road traffic injuries remain a major global public health and development challenge. The latest WHO Global Status Report on Road Safety estimates about 1.19 million deaths per year worldwide, making road crashes the leading cause of death for children and young people aged 5–29 years ("GSR on Road Safety" 2023). These deaths and serious injuries are strongly linked to the quality of road infrastructure. Because upgrading road networks is costly, governments and funding agencies increasingly rely on standardized risk assessment tools to prioritize where investments will have the greatest safety impact. The International Road Assessment Programme (iRAP) responds to this need through its Star Rating methodology, which converts coded roadway and roadside attributes into a Star Rating Score (SRS) for each 100-m road segment and road-user group (iRAP, 2021). These scores underpin star ratings and Safer Roads Investment Plans that influence large-scale spending decisions by national authorities and development banks.

Road safety risk assessment has increasingly shifted from reactive, crash-based evaluation toward proactive, model-based approaches that estimate infrastructure-related risk before severe crashes occur. Among these, composite risk and appraisal models play a central role in guiding investment decisions, benchmarking safety performance, and prioritizing interventions. A comprehensive overview of such approaches is provided by (Byaruhanga and Evdorides 2021), who systematically reviewed road safety investment appraisal frameworks and highlighted their importance in supporting evidence-based transport policy. The review emphasizes that many existing models rely on complex indicator structures and implicit assumptions, which may significantly influence outputs but are rarely subjected to formal uncertainty or sensitivity analysis.

Within this landscape, the International Road Assessment Programme (iRAP) has emerged as one of the most widely adopted infrastructure-based road safety assessment frameworks worldwide. The iRAP model integrates four core protocols risk mapping, star ratings, Safer Roads Investment Plans (SRIP), and performance tracking to assess and improve road safety while explicitly accounting for social and economic costs of road crashes. According to (Byaruhanga and Evdorides 2021) iRAP distinguishes itself by enabling economic appraisal of single or multiple countermeasures and by supporting large-scale implementation, having been applied in more than 100 countries across diverse geographical and socio-economic contexts.

Several applied studies have demonstrated the practical utility of iRAP as a road infrastructure risk assessment tool. (Murozi et al. 2022) evaluated the strengths and limitations of iRAP implementation and highlighted its ability to assess road safety even in contexts where reliable crash data are scarce. The authors emphasized that iRAP's reliance on observable roadway and roadside attributes allows proactive safety evaluation without historical accident records, which is particularly valuable in low- and middle-income countries. However, the study also identified significant drawbacks, including the high cost and time requirements of data collection, the large number of coded attributes at 100-m intervals, and the susceptibility of the process to coding errors and inconsistencies. They further discuss that multiple coding phases often introduce errors, necessitating repeated validation and extensive coding training. Case-study-based research has further reinforced the role of iRAP as a proactive safety assessment tool. (Uddin and Raihan 2023) applied the iRAP star rating methodology using the ViDA platform to assess a 10-km road segment in Bangladesh, observing effectiveness in countermeasure definition.

Similarly, infrastructure inspection-based studies such as (Daidone et al. 2023) have shown how iRAP methodologies can be integrated into systematic road network inspections. Their work highlights the consistency and standardization offered by iRAP-aligned inspections across large networks. However, the study primarily focused on methodological implementation and compliance, without addressing the sensitivity of resulting safety scores to variations or uncertainty in inspection data.

Beyond the iRAP domain, uncertainty and sensitivity analysis have been extensively explored in other infrastructure risk modelling contexts. (Allen et al. 2022) proposed a comprehensive framework combining Monte Carlo simulation and polynomial chaos expansion to quantify uncertainty and identify influential parameters in seismic risk models for road networks, demonstrated that a small subset of parameters such as fragility functions, capacity loss, and traffic volume dominate overall risk estimates. This study illustrates the value of uncertainty propagation and sensitivity analysis in enhancing model transparency and guiding targeted risk mitigation, yet such techniques have not been widely adopted in iRAP-based road safety assessment.

Considering the widespread adoption of the iRAP framework and the limited attention given to uncertainty propagation within its risk scoring process, the primary objective of this study is to systematically quantify and analyze the impact of input uncertainty on the iRAP vehicle road safety risk assessment model. The main innovation of this work is to move iRAP-based infrastructure assessment from a purely deterministic scoring procedure to a probabilistic, sensitivity-aware framework. We implement a fully programmable version of the vehicle-occupant SRS model and couple it with Monte Carlo and low-discrepancy Sobol sampling to generate statistically representative ensembles of road segments, capturing both typical and extreme combinations of coded attributes. On top of this, we perform a systematic uncertainty and global sensitivity analysis that quantifies not only how widely SRS values can vary under realistic input uncertainty, but also which specific attributes and crash-type factors dominate that variability. By further introducing a normalized variant of the SRS, in which attribute multipliers are placed on a common multiplicative scale, study disentangle structural model influence from the strong weighting choices embedded in the original iRAP factors. The resulting insights provide concrete guidance on which attributes deserve priority in data collection, coding, and infrastructure upgrades, and offer a principled basis for designing and validating AI-driven systems that automatically infer iRAP attributes from imagery and sensor data.

2. iRAP Vehicle-Occupant Star Rating Model

2.1 *Overview of the Star Rating framework*

iRAP provides a family of infrastructure-based models that estimate the relative risk of death and serious injury for different road users based on coded road attributes. For each 100-m segment, separate SRS are calculated for vehicle occupants, motorcyclists, pedestrians and bicyclists. These continuous scores are then grouped into five Star Rating bands from 1-star (highest risk) to 5-star (lowest risk) (iRAP, 2021). In this study we focus exclusively on the vehicle-occupant model. The input to the model is a set of categorical attributes describing road geometry, cross-section, roadside environment, intersection layout, traffic management and operating conditions. Examples include lane width, median type, or roadside object and distance, among others. These attributes are coded following the official iRAP specifications (iRAP, 2014).

2.2 Crash types and factor structure

For vehicle occupants, iRAP distinguishes several crash types that capture the main mechanisms of severe injury e.g. *Run-off-road (driver-side and passenger-side), Head-on (loss of control), Head-on (overtaking*), *Intersection crashes* and *Property-access crashes*. The vehicle-occupant SRS for a 100-m segment is obtained by summing the contribution of all relevant crash types:

$$SRS = \sum_{\{c \in C\}} CTS_c \qquad (1)$$

where C denotes the set of crash types and $\mathrm{CTS}_c$is the Crash Type Score for crash type c. The crash type score is modelled as a product of five factor groups:

$$\mathrm{CTSc = Lc \times Sc \times Vc \times Fc \times Mc} \qquad (2)$$

Where L_c (Likelihood factor) is effect of attributes linked to crash initiation (e.g. lane width, curvature, delineation, roadside distance and objects); S_c (Severity factor) is effect of features that influence impact severity (e.g. roadside hazards, skid resistance, presence of safety barriers); V_c (Operating speed factor) is the dependence on the prevailing operating speed for the segment; F_c (External flow influence factor) is effect of other traffic flows (e.g. intersecting traffic at intersections, opposing flow for head-on crashes) and M_c (Median traversability factor) is the probability that an errant vehicle can cross the median, relevant for run-off and head-on crash types (iRAP Factsheet-6). Each factor is itself composed of multiplicative attribute-specific risk multipliers. Denoting the set of coded attributes by $x = (x_1, \dots, x_p)$, we can write, for factor group $g \in \{L, S, V, F, M\}$,

$$g_{c(x)} = \prod_{\{j \in \{J\}_{\{c,g\}}\}} r_{\{c,g,j\}(x_j)} \qquad (3)$$

where $\mathcal{J}_{c,g}$ is the subset of attributes that contribute to factor group g for crash type c, and $r_{c,g,j}(x_j)$is the risk multiplier associated with attribute j taking the coded value x_j. For example, for head-on loss-of-control crashes, the Likelihood factor may include multipliers for lane width, curvature, delineation and roadside hazards, whereas for intersection crashes the Likelihood factor is dominated by intersection type, channelisation and side-road traffic volume (iRAP, 2025)

2.3 *Attribute risk factors and lookup tables*

The risk multipliers $r_{c,g,j}(x_j)$ are specified in iRAP's road-attribute fact sheets as discrete tables that map each category of an attribute (e.g. "physical median ≥ 20 m", "centreline", "barrier") to a numeric factor for each crash type and road user (iRAP Fact Sheets). For instance, the *median type* table assigns very low risk factors to raised or barrier-protected medians and very high factors to unprotected centre lines or traversable medians, reflecting the increased probability and severity of head-on crashes when vehicles can easily cross into opposing lanes. Similarly, the skid resistance table increases risk factors as surface condition degrades from "good" to "poor" or "very poor", and the delineation table penalizes segments with missing or inadequate markings and signage.

2.4 *Star Rating bands*

For interpretation and comparison with standard iRAP reporting, the continuous SRS values are finally mapped into discrete Star Rating bands. Following the vehicle-occupant bands used in previous iRAP applications, we adopt thresholds as given in Table1.

Table 1. Structure of the Vehicle-Occupant Risk Multiplier Lookup Table

Star Ratings	Ranges
5 stars	$0 \leq \text{SRS} < 2.5$
4 stars	$2.5 \leq \text{SRS} < 5.0$
3 stars	$5.0 \leq \text{SRS} < 12.5$
2 stars	$12.5 \leq \text{SRS} < 22.5$
1 star	$\text{SRS} \geq 22.5$

These bands provide an intuitive categorization of relative risk and are widely used by road authorities and development banks when setting performance targets (e.g. "≥ 3-star for all national highways"). In our analysis, SRS and star bands are computed for two simulation ensembles: a 10,000-segment random Monte Carlo sample, used mainly to validate the implementation, and a Sobol quasi–Monte Carlo ensemble with 32,768 segments, which forms the basis of the uncertainty and sensitivity results reported in the following sections. This setup allows us to quantify both the distribution of risk scores under uncertainty and the probability that a segment falls into each star band.

3. Monte Carlo Simulation Framework

Monte Carlo simulation is a numerical technique in which a model is evaluated for many randomly generated input combinations in order to approximate the distribution of its outputs (Harrison 2010). In this case, the "model'' is the iRAP vehicle-occupant scoring equation from Section 2, and the output of interest is the Star Rating Score (SRS). Each simulated road segment is defined by a vector of coded attributes (lane width, median type, etc.), and Monte Carlo simulation allows us to explore how SRS behaves over a large variety of possible road conditions.

Two selection methods are considered for generating these attribute combinations. First, in standard Monte Carlo, every attribute is sampled uniformly at random from its allowed iRAP codes, independently of the others. This produces N scenarios $\{x^{(i)}\}_{i=1}^{N}$ that cover the full design space without favouring any particular attribute level and serves as a simple reference ensemble.

Second, a Sobol quasi–Monte Carlo design, instead of independent random draws, it generates a low-discrepancy Sobol sequence in $[0,1]^{\mathrm{p}}$(where p is the number of attributes) and map each component to a discrete code by partitioning $[0,1]$ into equal intervals. Sobol sampling gives a more even coverage of the high-dimensional space and leads to smoother estimates of SRS statistics and sensitivity indices for the same number of model evaluations.

3.1 *Input variables*

The model inputs are the categorical road attributes used in the iRAP vehicle-occupant equations, e.g.: lane width (< 2.75 m, 2.75–3.25 m, ≥ 3.25 m), median type (none, painted centreline, physical median, safety barrier), skid resistance, road condition etc. For each attribute j, the set of allowed codes $\mathcal{V}_j$ is taken directly from the iRAP fact sheets and stored as a lookup table, as described in Section 2.3. In this study we treat attributes as independent inputs; the aim is to explore the full range of plausible combinations.

3.2 *Random Monte Carlo sampling*

As a baseline, we generate $10{,}000$ synthetic road segments using standard Monte Carlo sampling. For each attribute j and scenario i,

$$x_j^{(i)} \sim \text{Uniform}(\mathcal{V}_j), i = 1, \dots, 10{,}000 \qquad (4)$$

That is, each coded level for a given attribute is sampled with equal probability, independently across attributes and scenarios. This yields a heterogeneous ensemble of road segments that cover both typical and extreme combinations present in the iRAP lookup tables. We use these random ensembles to validate the implementation and to provide a reference distribution for SRS and star ratings.

3.3 *Sobol quasi-Monte Carlo sampling*

To obtain smoother statistics and more stable sensitivity estimates, we also use Sobol low-discrepancy sequences. For the iRAP model with p attributes, we generate a scrambled Sobol sequence of N = 32768 = 2^{15} points:

$$u^{(i)} \in [0,1]^p, i = 1, \dots, 32\,768.$$

Each component $u_j^{(i)}$ is then mapped to a discrete code for attribute j by:

$$k = \lfloor u_j^{(i)} K_j \rfloor, x_j^{(i)} = v_{j,\min\,(k+1,\ K_j)}, \qquad (5)$$

where $K_j = \mid \mathcal{V}_j \mid$ is the number of allowed levels for that attribute and $v_{j,\cdot}$ are the corresponding codes.

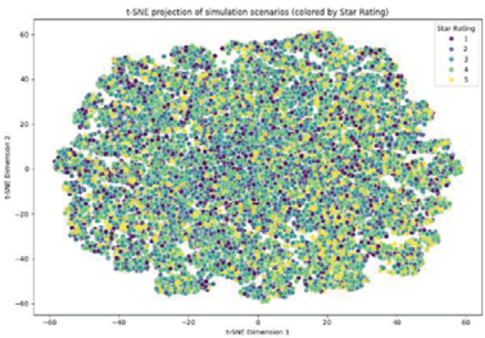

Fig.1. t-SNE Projection Colored by Star Rating

Figure 1 shows a 2D t-distributed Stochastic Neighbor Embedding (t-SNE) projection of simulation scenarios based on road attributes. Each point is a sampled scenario, colored by its iRAP Star Rating (1 star: 5007, 2 stars: 4605, 3stars: 9020, 4 stars: 8814, and 5 stars: 5322). The plot illustrates broad input space coverage and highlights how attribute combinations relate to safety performance. This construction preserves an approximately uniform frequency over the levels of each attribute while providing much better space-filling in the joint input space than purely random sampling. All Sobol experiments use the same fixed seed to ensure reproducibility. Using the Sobol quasi–Monte Carlo ensemble ($N = 32{,}768$), we also examine how the expected SRS varies across the categories of each attribute. Figure 2 summarises this effect in the form of a heatmap.

The heatmap in Figure 2 is computed directly from the Sobol ensemble. For each attribute (row) and each of its coded values (column), we select all simulated segments in which that attribute takes that value (while all other attributes are free to vary) and compute the mean SRS over those segments. The resulting mean SRS is shown as the colour intensity and numeric label of the corresponding cell. This provides a marginal view of how each attribute category is associated with higher or lower expected SRS.

The vehicle-occupant SRS is obtained as in Eq. (1). SRS$^{(i)}$is mapped to a 1–5 star band using the standard iRAP thresholds. For each rating store the attribute vector, crash type scores, SRS and star rating in a single table, which is then used as input to the uncertainty and sensitivity analyses in Section 4. Most simulations employ the original iRAP vehicle-occupant multipliers. In addition, we construct a normalized lookup table in which, for each attribute separately, the positive multipliers are rescaled in log-space so that their minimum and maximum map to a common multiplicative range (0.5–2.0), while preserving the ordering of categories. This yields an alternative "equal strength" SRS variant that we use later to study structural attribute influence independently of the very different weight ranges in the original factors.

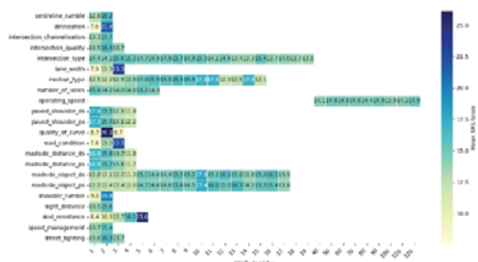

Fig.2. Heatmap of Mean SRS Scores by Attribute and Value

4. Sensitivity Analysis Framework

To understand how individual iRAP attributes influence the vehicle-occupant Star Rating Score (SRS), we treat the simulator as a function

$$\mathrm{SRS} = f(x_1, x_2, \dots, x_p), \qquad (6)$$

where x_j are the coded roadway and roadside attributes. Using the Sobol quasi–Monte Carlo ensemble of $N = 32\,768$simulated road segments generated in Section 3.3 (the 10,000-scenario random Monte Carlo run is only used for implementation checks and is not used in the sensitivity analysis), we perform global sensitivity analysis by computing several complementary measures between each attribute and the SRS. For each attribute x_j, we encode its categorical levels as integers and compute Pearson, Spearman and Kendall correlations between the vector of coded values $\{x_j^{(i)}\}_{i=1}^{N}$ and the corresponding SRS values $\{\mathrm{SRS}^{(i)}\}_{i=1}^{N}$. Below we briefly describe the techniques used in this study.

4.1 *Pearson and Spearman correlation*

Pearson's correlation coefficient measures the strength of a linear relationship between an attribute and the SRS. After encoding each attribute's categories as integers, values near +1/–1 indicate strong linear association and values near 0 indicate little linear trend. Pearson is simple and interpretable, but it assumes approximate linearity and is sensitive to outliers. While Spearman's rank correlation applies Pearson's formula to the ranks of the data instead of the raw values. It therefore captures any monotonic (consistently increasing or decreasing) relationship and is more robust to non-linearities and outliers. Previous comparative studies have shown that Pearson and Spearman behave differently under non-normal or heavy-tailed distributions, with Spearman often providing more stable estimates when outliers are present, whereas Pearson is preferable for light-tailed data (de Winter et al. 2016). A high Spearman coefficient means that as the attribute moves from "good" to "poor", the SRS tends to change consistently in one direction, even if the response is curved or step-like. Because our inputs are ordered risk levels, Spearman is a natural primary indicator, and Pearson serves as a complementary linear baseline. Figure 3 compares both measures in a single heatmap. For most attributes the sign of Pearson and Spearman is the same, confirming that the dominant effects are monotonic.

Delineation, lane width, road condition, skid resistance and shoulder rumble show the largest positive coefficients in both columns, with Spearman always larger in magnitude, indicating strong but slightly non-linear monotonic increases in SRS as these conditions deteriorate. Paved shoulders and roadside distance (driver and passenger side) exhibit negative coefficients, consistent with a protective effect as shoulders widen and hazards move further from the carriageway.

Overall, the joint Pearson–Spearman analysis shows that a small subset of attributes exerts a clear, predominantly monotonic influence on SRS, while many others contribute only weakly at the global scale.

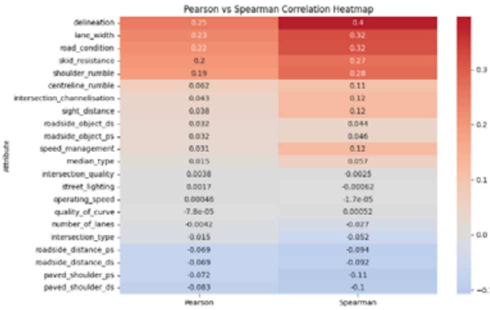

Fig.3. Heatmap of Pearson vs spearman correlation

4.2 *Mutual information*

While correlations focus on monotonic relationships, mutual information (MI) measures the overall dependency between an attribute and SRS without assuming linearity or monotonicity. We treat each attribute as a discrete variable (coded levels) and estimate the MI with the continuous SRS using the mutual_info_regression function from scikit-learn, with the attribute flagged as discrete and the default k-nearest-neighbour estimator. MI is always non-negative: a value of 0 means that, up to estimation noise, the attribute and SRS are independent, whereas larger values indicate stronger dependence. MI has no fixed upper bound and is interpreted relatively: for example, an attribute with MI ≈ 0.08 carries roughly twice as much information about SRS as one with MI ≈ 0.04. In the analysis we therefore use MI primarily to rank attributes by their information content with respect to SRS.

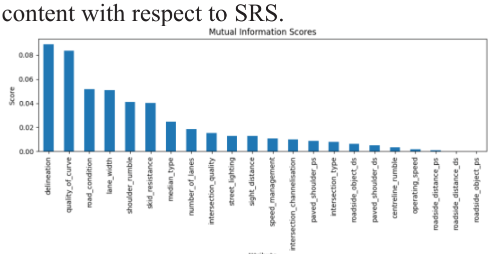

Fig.4. Bar chart of Mutual information scores

In Figure 4, MI provides a consistent but slightly richer picture than correlations. Delineation and quality of curve have the highest MI values, followed closely by road condition and lane width, confirming that these geometric and guidance-related attributes carry the most information about SRS. Shoulder rumble and skid resistance also show substantial MI, indicating that surface condition and run-off protection meaningfully reduce uncertainty in the score. Medium MI values for median type, number of lanes, intersection quality and street lighting suggest that these factors still influence SRS, but less strongly than the top group. At the lower end, attributes such as paved shoulders, roadside distance/objects, centreline rumble and operating speed have very small MI, implying that, under our sampling scheme and current risk factors, they add little additional information about SRS beyond what is already captured by the more influential attributes.

4.2 Kendall's tau

Kendall's tau is another rank-based measure that looks at pairwise concordance: for all pairs of segments, it checks whether higher attribute codes tend to be paired with higher (or lower) SRS. It is more conservative than Spearman and often less sensitive to noise in small samples (El-Hashash and Shiekh 2022). A higher absolute tau indicates a more consistent monotonic relationship between an attribute and SRS.

In Figure 5, Kendall's tau yields a pattern very consistent with the Spearman results but with smaller magnitudes, as expected for this more conservative measure. Delineation, lane width, road condition, shoulder rumble and skid resistance again show the strongest positive tau values, indicating a very stable tendency for poorer levels of these attributes to be associated with higher SRS across segment pairs. Speed management, sight distance, intersection channelisation and centreline rumble have moderate positive tau, suggesting a weaker but still systematic monotonic effect. Overall, Kendall's tau largely confirms the ranking obtained from Spearman, reinforcing the conclusion that a small group of geometric, surface and guidance attributes are the primary monotonic drivers of the vehicle-occupant SRS.

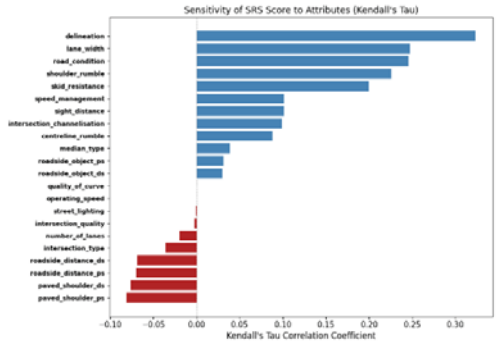

Fig.5. Kendall's Tau sensitivity scores

Taken together (Figure. 6), the four measures give a very consistent picture of which attributes matter most for the vehicle-occupant SRS. Pearson, Spearman and Kendall all agree that delineation, lane width, road condition, skid resistance and shoulder rumble are the dominant risk-increasing factors, with positive coefficients of comparable magnitude, while paved shoulders and greater roadside distance on both sides show stable negative correlations, confirming their protective effect. Mutual information largely supports this ranking and further emphasises delineation, curve quality, surface condition and lane width as the attributes that carry the most information about SRS, whereas variables such as street lighting, operating speed, number of lanes and intersection quality consistently exhibit very low scores across all metrics.

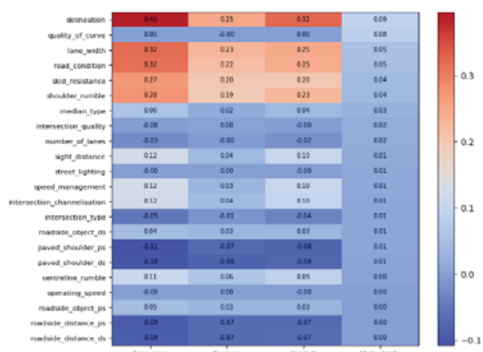

Fig.6. Combined sensitivity metrics for SRS

5. Conclusion

The study reframed the iRAP vehicle-occupant Star Rating Score as a probabilistic quantity by coupling the official SRS equations with Monte Carlo and Sobol quasi–Monte Carlo simulation. Using large ensembles of synthetic road segments, quantifies how uncertainty in coded infrastructure attributes propagates to the SRS and corresponding star bands, and evaluated global sensitivity using Pearson, Spearman, Kendall correlations and mutual information.

Across all metrics, a small group of attributes consistently dominated: poor delineation, narrow lanes, degraded road condition and skid resistance, and the absence of shoulder rumble strips strongly increased SRS, while paved shoulders and greater roadside clear zones reduced it. Many other coded variables showed only weak global influence. These findings provide a clear priority list for data collection and low-cost infrastructure improvements and indicate which attributes AI-based coding systems must predict most reliably. Future work will extend the analysis to other iRAP user groups, cost analysis and to network-specific attribute distributions, moving toward fully uncertainty-aware, automated infrastructure risk assessment.

Acknowledgement

This work has been funded by grant RYC2021-033560-I funded by MCIN/AEI/ 10.13039/501100011033 and by European Union NextGenerationEU/PRTR and by grant ED431F 2024/02 funded by Xunta de Galicia, Spain-GAIN. Funding for open access charge: Universidade de Vigo/CISUG.

References

Allen, Eduardo, Alondra Chamorro, Alan Poulos, Sebastián Castro, Juan Carlos de la Llera, and Tomás Echaveguren. 2022. “Sensitivity Analysis and Uncertainty Quantification of a Seismic Risk Model for Road Networks.” Computer-Aided Civil and Infrastructure Engineering 37 (4): 516–30. https://doi.org/10.1111/mice.12748.

Byaruhanga, Chris Bic, and Harry Evdorides. 2021. “A Systematic Review of Road Safety Investment Appraisal Models.” Cogent Engineering 8 (1): 1993521. https://doi.org/10.1080/23311916.2021.1993521.

Daidone, Lauragrazia, Enrico Pagliari, Lucia Pennisi, Edoardo Caporali, Edoardo Mazzia, and Paola Tiberi. 2023. “Road Infrastructure Inspections to Assess the Road Network According to the iRAP/EuroRAP Methodology.” Transportation Research Procedia, AIIT 3rd International Conference on Transport Infrastructure and Systems (TIS ROMA 2022), 15th-16th September 2022, Rome, Italy, vol. 69 (January): 743–50. https://doi.org/10.1016/j.trpro.2023.02.231.

El-Hashash, Essam F., and Rega Hassan Ali Shiekh. 2022. “A Comparison of the Pearson, Spearman Rank and Kendall Tau Correlation Coefficients Using Quantitative Variables.” Asian Journal of Probability and Statistics, October 18, 36–48. https://doi.org/10.9734/ajpas/2022/v20i3425.

Factsheet-6. n.d. “iRAP, 2021.” Accessed December 27, 2025. https://www.scribd.com/document/558761171/IRAP-Model-Factsheet-6-Star-Rating-Score-Equations.

“GSR on Road Safety.” 2023. https://www.who.int/publications/i/item/9789240086517.

Harrison, Robert L. 2010. “Introduction To Monte Carlo Simulation.” AIP Conference Proceedings 1204 (January): 17–21. https://doi.org/10.1063/1.3295638.

“iRAP, 2025.” 2025. The Road Safety Foundation. https://roadsafetyfoundation.org/irap-tools-and-methodology/irap-process-steps/.

“iRAP Methodology Fact Sheets.” n.d. iRAP. Accessed December 27, 2025. https://irap.org/methodology/.

Murozi, Ainatul-Fatima Md, Siti Zaharah Ishak, Fatin Najwa Mohd Nusa, Alvin Poi Wai Hoong, and Sonya Sulistyono. 2022. “The Application of International Road Assessment Programme (iRAP) as a Road Infrastructure Risk Assessment Tool.” 2022 IEEE 13th Control and System Graduate Research Colloquium (ICSGRC), July, 237–42. https://doi.org/10.1109/ICSGRC55096.2022.9845149.

“Star Ratings.” 2021. iRAP. https://irap.org/rap-tools/infrastructure-ratings/star-ratings/.

Uddin, Md. Imran, and Md Asif Raihan. 2023. “Proactive Safety Assessment of a Road Using iRAP Tool: A Case Study.” AIP Conference Proceedings 2713 (1): 040012. https://doi.org/10.1063/5.0131224.

Winter, Joost C. F. de, Samuel D. Gosling, and Jeff Potter. 2016. “Comparing the Pearson and Spearman Correlation Coefficients across Distributions and Sample Sizes: A Tutorial Using Simulations and Empirical Data.” Psychological Methods (US) 21 (3): 273–90. https://doi.org/10.1037/met0000079.